



Characterization of Au/Au, Au/Ru and Ru/Ru ohmic contacts in MEMS switches improved by a novel methodology

A. Broue, J. Dhennin, F. Courtade, C. Dieppedale, Patrick Pons, X. Lafontan, Robert Plana

► To cite this version:

A. Broue, J. Dhennin, F. Courtade, C. Dieppedale, Patrick Pons, et al.. Characterization of Au/Au, Au/Ru and Ru/Ru ohmic contacts in MEMS switches improved by a novel methodology. *Journal of Micro/Nanolithography, MEMS, and MOEMS*, Society of Photo-optical Instrumentation Engineers, 2010, 9 (4), pp.041102-1 / 041102-8. <hal-00624780>

HAL Id: hal-00624780

<https://hal.archives-ouvertes.fr/hal-00624780>

Submitted on 19 Sep 2011

HAL is a multi-disciplinary open access archive for the deposit and dissemination of scientific research documents, whether they are published or not. The documents may come from teaching and research institutions in France or abroad, or from public or private research centers.

L'archive ouverte pluridisciplinaire **HAL**, est destinée au dépôt et à la diffusion de documents scientifiques de niveau recherche, publiés ou non, émanant des établissements d'enseignement et de recherche français ou étrangers, des laboratoires publics ou privés.

Characterization of Au/Au, Au/Ru and Ru/Ru ohmic contacts in MEMS switches improved by a novel methodology

Adrien Broue^{*a,b,c}, Jérémie Dhennin^a, Frédéric Courtade^d, Christel Dieppedale^e, Patrick Pons^{b,c},
Xavier Lafontan^{a,f}, Robert Plana^{b,c}

^aNovaMEMS ; c/o CNES 18 Avenue E. Belin 31401 Toulouse cedex 9, France

^bCNRS ; LAAS ; 7 avenue du colonel Roche, F-31077 Toulouse, France

^cUniversité de Toulouse ; UPS, INSA, INP, ISAE ; LAAS ; F-31077 Toulouse, France

^dCNES ; 18 Avenue E. Belin 31401 Toulouse, France

^eCEA-LETI, Minatec ; 17 rue des Martyrs, 38054 Grenoble Cedex 9, France

^fINTESENS ; 10 Avenue de l'Europe 31520 Ramonville, France

ABSTRACT

Comparisons between several pairs of contact materials have been done with a new methodology using a commercial nanoindenter coupled with electrical measurements on test vehicles specially designed to investigate the micro-scale contact physics. Experimental measurements are obtained to characterize the response of a 5 μm^2 square contact bump under electromechanical stress with increased applied current. The data provide a better understanding of micro-contact behaviour related to the impact of current at low- to medium-power levels. Contact temperature rise is observed, leading to shifts of the mechanical properties of contact materials and modifications of the contact surface. The stability of the contact resistance, when the contact force increases, is studied for contact pairs of soft (Au/Au contact), harder (Ru/Ru contact) and mixed material configuration (Au/Ru contact). An enhanced stability of the bimetallic contact Au/Ru is demonstrated considering sensitivity to power increase, related to creep effects and topological modifications of the contact surfaces. These results are compared to previous ones and discussed in a theoretical way by considering the temperature distribution around the hottest area at the contact interface.

Keywords: MEMS, Switch, Micro contact, Contact material, Contact temperature, Creep, Gold, Ruthenium

1. INTRODUCTION

From DC up to tens of giga hertz, the bandwidth of RF MEMS switch specifications is spreading more and more. But is the challenge reachable for ohmic contact switches? Even if some successful companies now propose some of these breakthrough-told technologies, the gap is still large between the low TRL (Technology Readiness Level) academic demonstrations and the commercially available switches. Several reasons can be exposed to account for this, and one of them is probably the lack of adapted tools to investigate the physics occurring at such a tiny scale. Research on contact characterization for microelectromechanical system (MEMS) switches has been driven by the necessity to reach a high-reliability level for micro-switch applications. One of the main failure observed during aging of the devices is the increase of the electrical contact resistance. The key issue is the electromechanical behaviour of the materials used at the contact interface when the current is flowing through the contact asperities. In addition, design of MEMS switches is widely diversified and few comprehensive investigations of micro-contact physics have been reported on a single type of contact. For ohmic contact switches, the main issue is to control precisely the contact pressure and the corresponding temperature. These two parameters are interdependent as soon as some DC or RF signal is flowing through the contact.

As a consequence, new characterization techniques have been recently developed in order to measure the contact resistance functions of the load applied and the contact deformation. Moreover, a precise monitoring of the current intensity and of the associated potential drop is useful to get rid of any parasitic resistance using cross rod configuration.

*adrien.broue@novamems.com; phone +33 5 6127 4688; fax +33 5 6127 4732; novamems.com

Works on FEM structural-contact analysis were reported at Memswave 2009 where temperature was studied at the contact interface [1]. Fortini presented a nanoscale comparison of Au and Ru contact behaviour using molecular dynamics simulation [2]. Experimental characterizations using nanoindenter [3], piezo actuator [4] and atomic force microscope (AFM) [5] were published by several researchers, to investigate the behaviour of Au and Au-Ni alloys as contact materials by mechanical actuation with increasing force. To our knowledge, the micro-scale heating effects on the contact material are not fully understood. However these phenomena are key issues for the designers to understand the capability of the contact to sustain the current before reaching critical temperature values for the used material [1]. In this paper, the analysis of the impact at low to medium power level on Au, Ru and Au/Ru based RF MEMS contacts differs from previous works as the study of the power sensitivity is based on experimental results. In addition, these tests are performed using the dynamic control module of the nanoindenter (DCM), which allows a higher resolution testing. This apparatus is coupled with an environmental chamber to control both temperature and humidity. In addition, the tests are simplified by measuring the DC contact resistance instead of the S-parameters.

This work proposes a method to compare the behavior of three couples of contact materials. This paper is organized as follows. The section 2 is an overview of the micro-contact theory. In section 3, the experimental apparatus and device are described. Experimental results are presented in section 4. These results are compared to previous ones and discussed in a theoretical way by considering the temperature distribution around the hottest area at the contact interface in section 5, followed by the summary and conclusions in section 6.

2. MICRO CONTACT THEORY

The electromechanical behaviour of the contacting surfaces during switching depends on several mechanical and operating parameters such as thermal (σ_t) and electrical (σ_e) conductivity of contact materials, mechanical properties of the contact spots (E and H), roughness (Ra), adhesion energy of contact surfaces (γ), mechanical stiffness (k), humidity (Rh), contact voltage (V_c), contact force (F_c) (cf. Figure 1). The key issue is the stability of the contact surfaces through aging: the electrical, topological and mechanical properties have to be maintained the longest time.

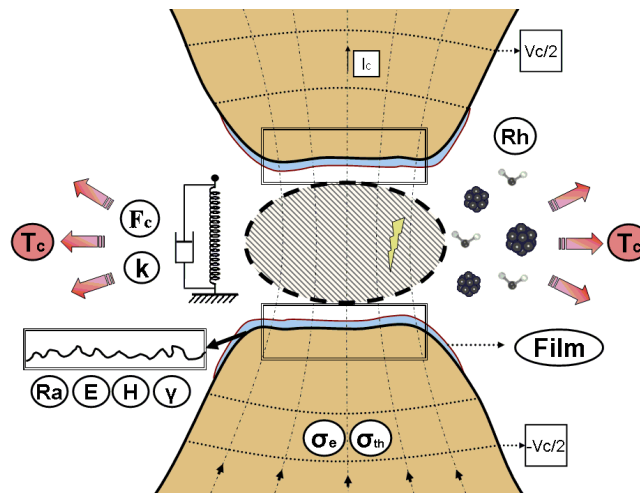


Figure 1 : Complexity of micro-contact failure mechanisms

2.1 Analytic models

First, the micro-contact physically differs from the macro-contact due to the roughness of the contact surface. Only high points on each surface come in contact. Thereby the effective contact area, named asperities or a-spots, is largely smaller than the apparent one.

To simplify the model, the contact resistance (R_c) is assumed to be mainly governed by the constriction resistance as the current flow is constricted through the small asperities leading to the electrical contact ie. the electrical contact is considered strictly ohmic. This electrical resistance is directly linked to the constriction of current lines between both contacts. This constriction of current causes a local increase of the current density and tends to increase the electrical potential drop between the two sides of the contact.

Thus the expression of this constriction resistance, so called Maxwell resistance $R_{Maxwell}$, can be written for a single circular contact spot of radius a as [6]:

$$R_{Maxwell} = \frac{\rho}{2a} \quad (1)$$

Where ρ is the resistivity of the contact material. During the first contact establishment between the two surfaces, the load applied is generally higher than the yield stress of the contact material. Thus the deformation of the contact asperities is considered to be predominantly plastic. The contact area and the contact load can be linked to the radius of the contact spot a using Abbott and Firestone's plastic contact model [6].

$$a = \sqrt{\frac{A_c}{\pi}} = \sqrt{\frac{F_c}{H\pi}} \quad (2)$$

Where A_c is the contact area, F_c the contact force and H the Meyer hardness of the softer material. Secondly, it's necessary to keep in mind that, generally, the current flows by multiple asperities due to the surface roughness. The easier approach consists in considering that the whole conductance is the sum of conductances of the multiple contact spots with varying sizes. The effective contact resistance can be obtained as a first approximation by summing all the contact radii of all the individual asperities as the effective contact radius a_{eff} of the effective contact area A_{eff} . This effective contact radius can be substituted into (1) and (2) to take into account the multiple asperity feature of the micro contact.

Because of tiny contact spot size due to small contact force available in micro-switches, mechanical, electrical and thermal properties shift from bulk to a specific physics of thin films lead by the geometry of the asperities. For example, heating of the contact spots is extremely localized when the current flows through the contact, whereas the device level remains at room temperature [7]. The highest contact spot temperature T_c called supertemperature T_Θ has already been expressed by Holm as a function of the contact voltage V_c [6] :

$$T_\Theta = \sqrt{\frac{\Gamma(K)R_{Maxwell}V_c^2}{R_c 4L}} + T_0 \quad (3)$$

Where $L=2.45 \times 10^{-8} \text{ W}\cdot\Omega/\text{K}^2$ is the Lorentz constant, $\Gamma(K)$ a slowly varying Gamma function and T_0 the ambient temperature. By considering that electrical contact is strictly ohmic, this equation becomes:

$$T_\Theta = \sqrt{\frac{V_c^2}{4L}} + T_0 \quad (4)$$

Eq. (3) is obtained from the Wiedemann-Franz law for a conductor heated by the current produced by the voltage V_c between two arbitrary isotherms with the temperature T_0 : the assumption is made that the thermal and electric currents obey similar laws thus with symmetric contacts the generated heat flows in the same path as the electric current.

2.2 Reliability of micro-contact

The second important point to be addressed is the reproducibility of the contact resistance over the actuations, and thus along its whole lifetime (cf. Figure 2). The reliability of the switch depends on its ability to withstand some degradations occurring at the contact interface. Three types of phenomena can be studied: the mechanical (cold welding, strain hardening), electrical (arcing, hot welding, annealing) and chemical ones (formation of insulating films at the extreme surface), all inducing modifications of the topological, mechanical and electrical properties of the contact.

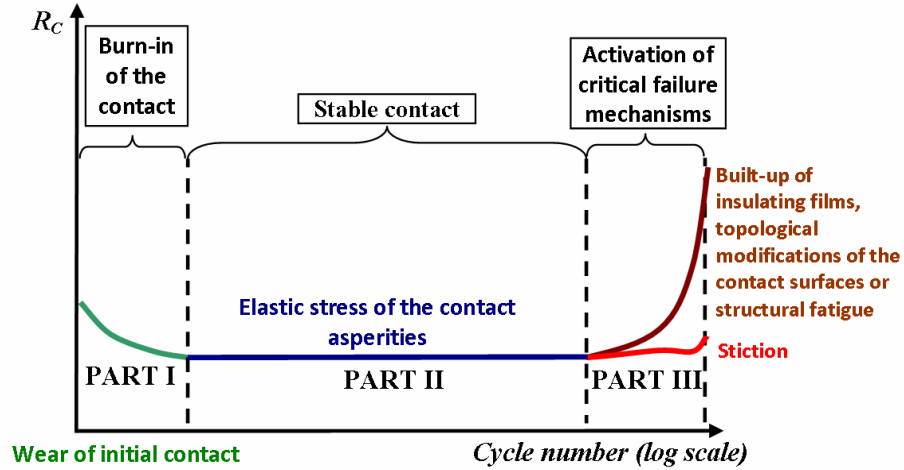


Figure 2 :Typical lifetime of micro switches leading to contact failure

As the experimental set-up developed here can be used for studying the fundamental physics of the micro-contact, the understanding of potential failure mechanisms can be made easier if the effort is put upon the identification of the key parameters for each mechanism. In addition, the contact temperature (T_c) of contact a-spots could be linked with the contact force depending on the contact voltage [4]. Indeed the plastic deformation of the asperities during the contact formation proceeds more rapidly when the softening temperature is reached [2]. Thus the effective contact area increases inducing a drop of the contact resistance. However the softening of the metal at the asperities of contact reduces the strain hardening of the a-spots and could accelerate the aging of the contact by the activation of thermal failure mechanisms. Therefore the softening temperature of contact metals is probably one of the most important critical parameter and it has to be study for reaching a stable and low contact resistance.

2.3 Contact material focus

The performance of the electrical contact in a MEMS switches is strongly linked with the materials used to perform the contact. The mechanical and electrical properties of the contact material will govern the behaviour of the contact resistance versus the contact load applied. It is important to find the best compromise between mechanical and electrical performances to reach the best reliable operations. The contact must have excellent electrical conductivity for low loss, high melting point to handle power, appropriate hardness to avoid stiction phenomenon and chemical inertness to avoid oxidation [8]. Furthermore, the used contact material influences the contact reliability because of material-dependent contact degradation through mechanical wear, fretting, creep, localized hardening, arcing, etc.

3. EXPERIMENTAL TECHNIQUES

3.1 Experimental set-up description

The test described in this paper is based on methods combining a nanoindenter and a high resolution source meter for the determination of the electrical contact resistance versus the contact force and the displacement of the free standing part of the contact. Nanoindentation is firstly designed for material characterization, which is based on the “displacement vs. load” curve obtained by driving a tip into the test material and by monitoring the applied load and the resulting displacement [9]. In our test bench, the nanoindenter’s spherical tip is used as a mechanical actuator. The actuation load is thus reproducible and known with a good accuracy, two points which remain hard to achieve with the actual actuations (for example, electrostatic actuation forces often drift due to dielectric charging [10]).

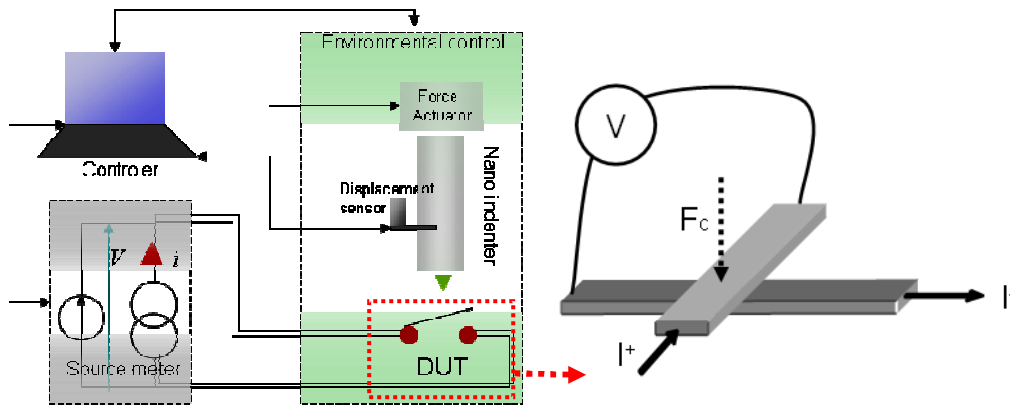


Figure 3 : Principle of the electrical test performed with a nanoindentation tip

Once the bridge is correctly located under the column of nanoindentation, the tip is brought in contact with the surface of the mobile electrode, and then lowered until mechanical and electrical contact between the bridge and the line. The stiffness of the membrane can be measured in this step [11]. From this moment on, the applied load corresponds to the actuation load of the contact. A schematic view of the set-up can be seen on Figure 3.

The main difficulty for applying a load on test vehicles remains the accurate location of the tip above the contact. This issue has been here overcome by the use of a nanopositioning table achieving a 20nm X-Y resolution in a defined 100 μ m-side square. Thus, a pseudo-AFM scan is performed by probing the surface with a fixed stiffness of contact between the tip and the surface. An accurate location can then be reached on the scan (cf. Figure 4).

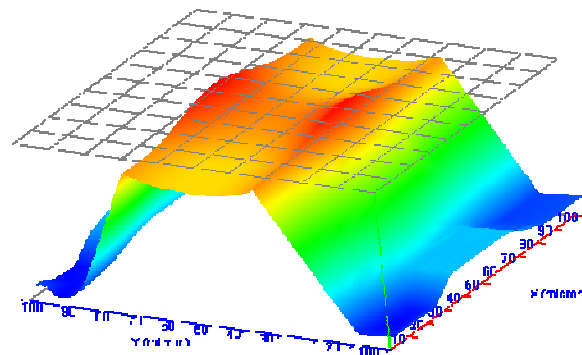


Figure 4 : Picture of the scan performed with the nanoindenter on the test structure

The electrical measurements are performed by the use of a four-wires probe: a current flow I_C is applied and the potential drop V_C is independently measured. This method for measuring contact resistance is the same method used in crossed rod contact resistance measurements of Holm [6]: only the contact resistance is measured independently of the voltage drop in the supply wires and access paths. Moreover the environmental chamber allows the control of the temperature of the DUT and of the relative humidity Rh .

3.2 Test vehicle description

Specific test vehicles have been designed for contact analysis, enhancing the extraction of characteristic curves and making possible the comparison between different contact shapes or materials. As illustrated in Figure 5, the tested device is composed of a bridge suspended over a contact line.

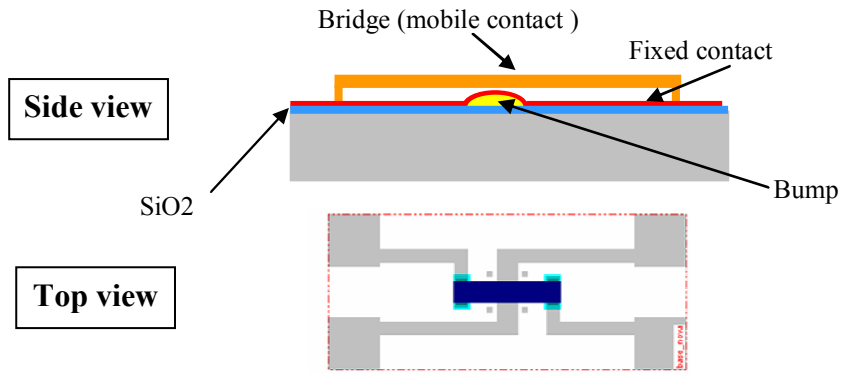


Figure 5 : Scheme of the test structures

A $5\mu\text{m}\times 5\mu\text{m}$ square bump is processed underneath. Three kinds of test structures, described in table 1, are used.

Table 1 - Description of the test structures

Nomenclature	Contact materials	Measured bridge stiffness
P10	<i>Au-to-Au</i>	480 N/m
P09	<i>Au-to-Ru</i>	515 N/m
P05	<i>Ru-to-Ru</i>	225 N/m

Two contact materials are tested (cf. table 2): Au, which is the most popular material for electrical contact because of its high bulk conductivity, low contact resistance even at small contact forces, its high oxidation resistance, its low propensity to form alien surface films [11] and its fabrication compatibility with MEMS fabrication methods.

Table 2 - List of properties of switch contact metals

Contact materials	Electrical conductivity ($\text{m}\Omega^{-1}\cdot\text{mm}^{-2}$) [9]	Softening temperature ($^{\circ}\text{C}$)	Melting temperature ($^{\circ}\text{C}$) [9]	Boiling temperature ($^{\circ}\text{C}$) [9]	Estimated hardness (GPa) [9]
Au	45.7	~ 100 [6]	1063	2966	~ 1.6
Ru	14.9	~ 430 [12]	2450	4900	~ 10.1

However, Au is a soft material, thus the probability of getting large modifications of the contact surface during aging is really high. Furthermore, Au is susceptible to contact wear, which affect the contact performance. This is the reason why new contact metals have to be introduced, as Ru. It is much harder than pure Au or any Au alloy. Ru/Ru contact and Ru/Au contact may provide better resistance stability in spite of a higher bulk resistivity [14]. The test structures were stored in clean N_2 what could slow down environmental contamination of the contact surfaces but gradual contamination accumulation still occurred.

3.3 Test description

A campaign of tests has been made on the test vehicles described in the previous paragraph. These studies are focused on the self heating of the contact with increased levels of current flowing through the contact at low- to medium-power levels. Contact resistance versus contact force curves are obtained, up to $145\mu\text{N}$ for Au/Au and Ru/Au, and up to $200\mu\text{N}$ for Ru/Ru. The contact super-temperature is then extracted. The measurements are performed by sweeping the contact current from 1 mA to 100 mA and measuring the contact voltage in a cold-switching way. The load rate is about $1\mu\text{N/s}$ to allow the contact deformation to reach a steady-state. The following results are based on the same 11 successive tests

for the three pairs of contact materials (Au/Au, Ru/Au and Ru/Ru). In addition dedicated validation tests and FEM modelling have already assessed the introduced methodology [15].

4. EXPERIMENTAL RESULTS

This part of the paper compares the heating of micro-contacts with various pairs of contact materials by increasing the contact current. To further examine the heating effect on contact resistance, the study is focused on the contact temperature when the maximum contact load is reached. The methodology consists on measuring the contact voltage while imposing the current flowing through the contact. The series of tests described previously will be used to compare the impact of increased contact current on the three test vehicles.

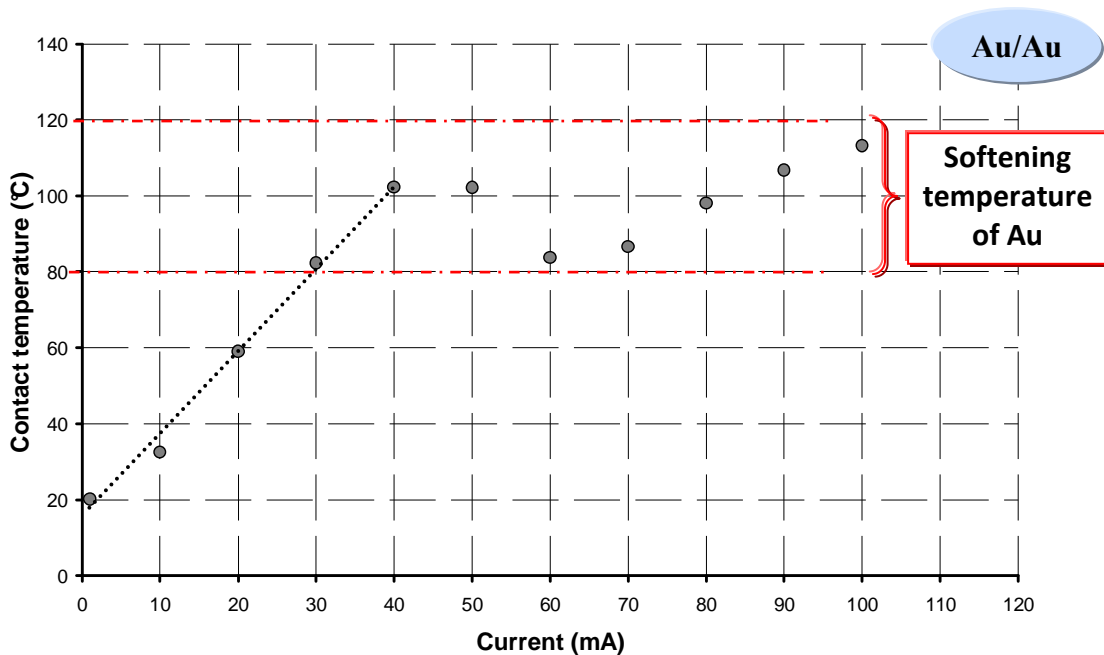


Figure 6 - Contact temperature versus the contact current for Au/Au contact

Figure 6 shows the contact temperature as a function of the contact current for Au/Au contact. The contact temperature is calculated thanks to the contact voltage measured across the contact (Eq.4). Thus the behaviour of the temperature across the contact can be observed while the level of current is increasing.

The published softening temperature for gold contact is $\sim 100^{\circ}\text{C}$, corresponding to a contact voltage of 70-80 mV for contact near room temperature [6]. When the contact current is increased after reaching the softening temperature from 40 mA, the contact resistance continues to decrease keeping the contact temperature roughly constant. The contact temperature increases with a constant slope from 1mA to 40mA. At this point the contact temperature stops to increase and fluctuates between 80°C and 120°C (65 mV to 75 mV). This temperature seems to be stabilize while the power within the contact rises.

The same behaviour is partially observed for the other symmetrical contact Ru/Ru. Indeed the published temperature for ruthenium contact is $\sim 430^{\circ}\text{C}$, corresponding to a contact voltage of 200 mV for contact near from room temperature [12]. When the softening temperature is reached, the contact temperature does not depend strongly on contact current at high current levels. Beyond this value, the contact temperature is unstable even though it seems to oscillate around the softening temperature.

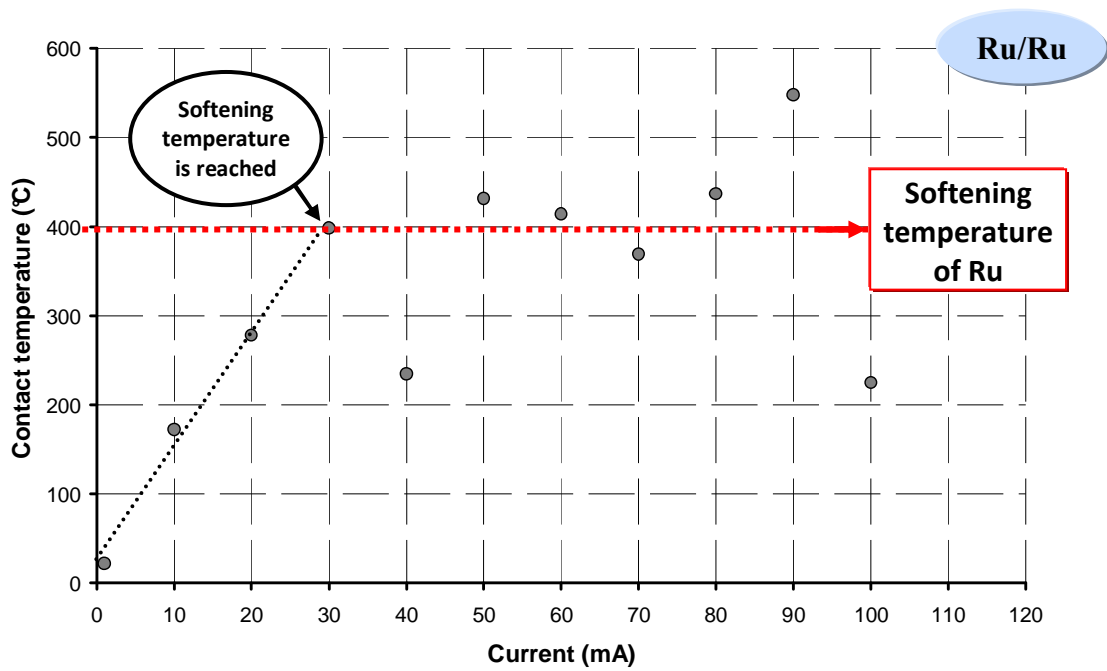


Figure 7 - Contact temperature versus the contact current for Ru/Ru contact

The behaviour for the asymmetrical contact Au/Ru defers from the two others because of the different materials in the both part of the contact.

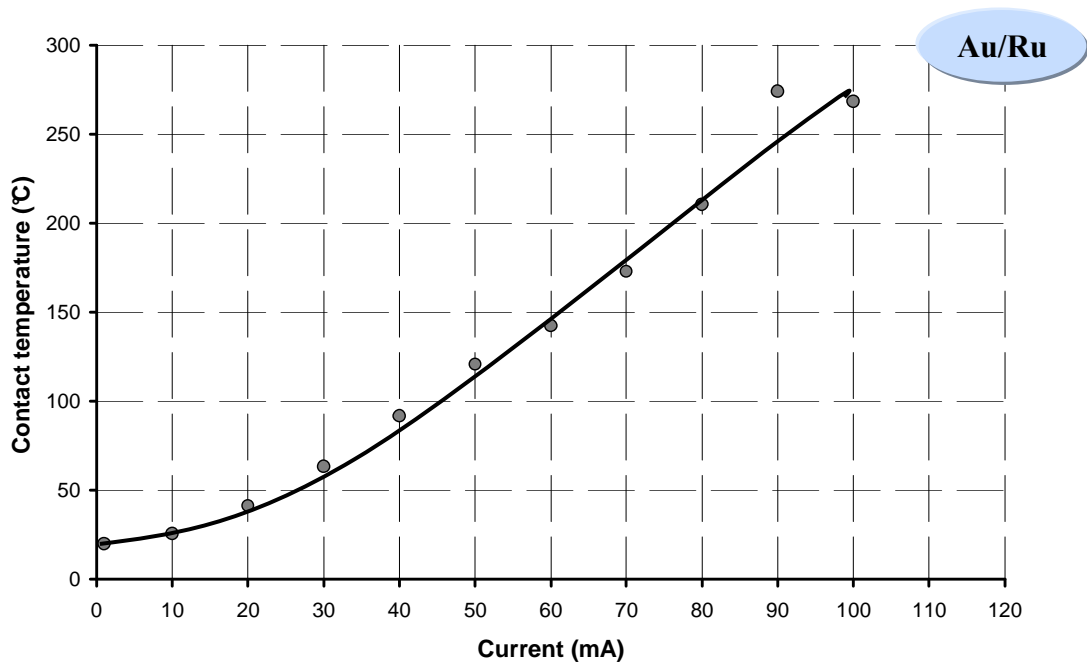


Figure 8 - Contact temperature versus the contact current for Au/Ru contact

As shown in Figure 8, the contact temperature increases with the current level without reaching a maximum. The temperature distribution within the contact constriction has change in comparison with a contact with the same contact metal. In the case of Au/Ru contact, the conductivities of the both material are different yielding to the apparition of thermoelectric effects.

5. DISCUSSION

The previous section pointed out the dissimilar behaviours of symmetrical and asymmetrical contact materials. The Figure 9.a is a scheme which represents both contact members of the same material M1. The assumption that the electrical and thermal currents flow in the same paths is always supported as described by the Wiedeman-Franz law. T_0 is the bulk temperature in the both members of the contact. A_0 corresponds to the section of the extreme contact interface across which no heat flows. The highest temperature T_θ is localized at the contact interface where the contact voltage V_C is equal to 0V (Holm's convention [6]). The distribution is symmetric around the hottest contact spot precisely localized at the intersection between the both part of the contact.

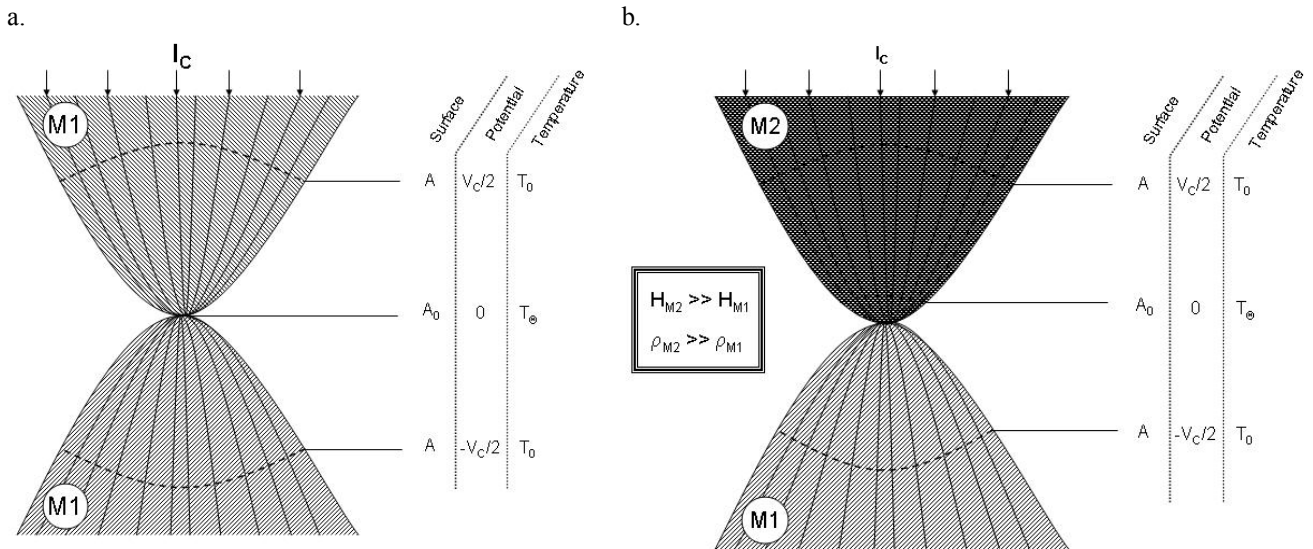
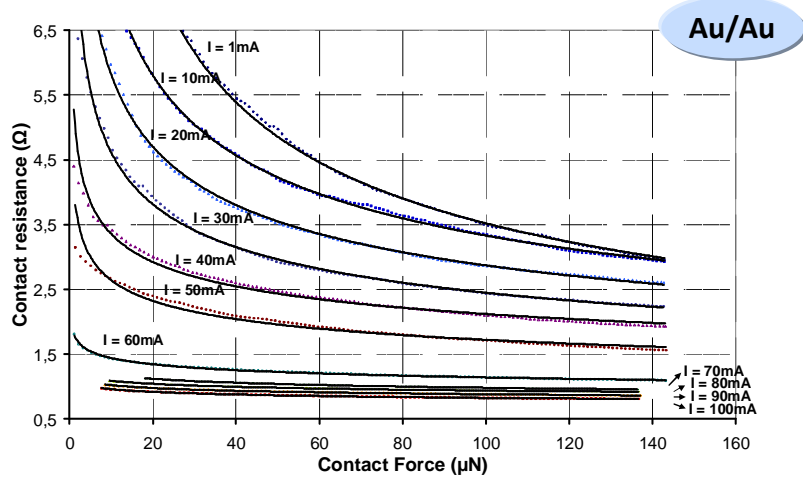


Figure 9 – Temperature distribution a) in a symmetric constriction b) in the constriction of a contact between two metals M1 and M2 with different conductivities

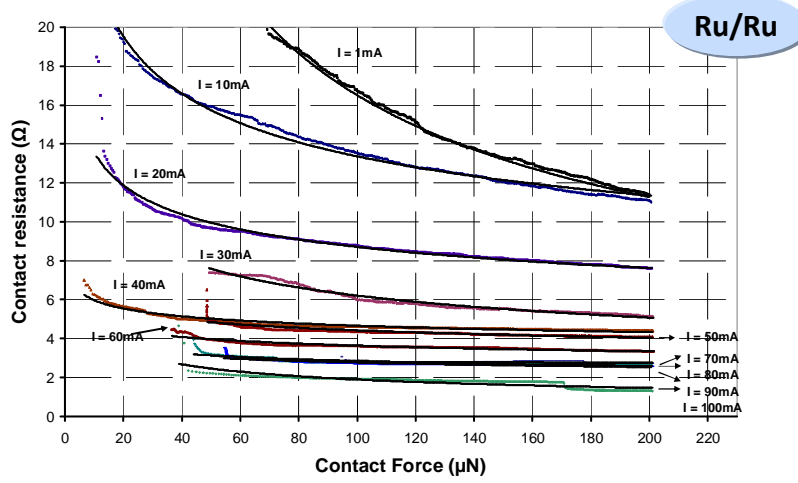
The Figure 9.b illustrates the temperature distribution at the contact constriction between two metals M1 and M2 with different conductivities. The distribution around the hottest area at the contact interface has changed because of the different nature of the both contact parts. Thus there is a change in the average distance of the thermoelectric heat flow. The maximum temperature T_θ is located within the poorer conductor so the positions of interface around the contact between the metallic members M1 and M2 [6].

Thus the phenomenon observed in the Au/Ru contact can be explain as the maximum contact temperature calculated in the Figure 8 is thus located in the ruthenium member of the contact. The maximum contact temperature obtained is about 274°C, that is to say less than the softening temperature. The conclusion is that the contact temperature of the asymmetric contact is more stable because the softening temperature is theoretically not reached for the same contact current.

a.



b.



c.

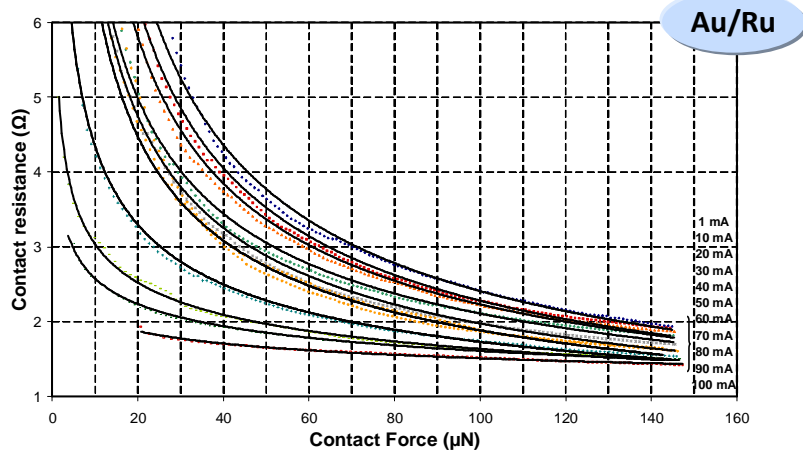


Figure 10 - Contact resistance versus contact force as a function of the current flowing through the contact for a) Au/Au, b) Ru/Ru and c) Au/Ru contacts

Measured contact force versus contact resistance curves for Au/Au, Ru/Ru and Au/Ru contacts are shown in Figure 10. When contact is made between two metallic electrodes, the contact area is very low at first and the resistance is high and unstable. At a certain minimum force, depending on the material under investigation, a significant reduction of the resistance occurs. At higher forces, the contact is stable and the resistance decreases slightly with further increasing force until a saturated regime. The contact resistance reduction with increased current is thermally induced.

The stability of the contacts is investigated in terms of dispersion of R_C versus F_C curves. The conclusion is that Au/Ru is clearly the more stable contact at the maximum contact load. Indeed, the contact temperature increases with the current until reaching the softening temperature for Au/Au contact and for Ru/Ru contact. The contact hardness is subsequently reduced because of the annealing of the contact. Then the roughness of the contact is lowered after softening of the surfaces. Thereby, the deformation of the contact asperities is higher with increased current making easier the breakdown of residual insulating films, and enlarging the total contact area. However, the variation of the contact resistance is determined by a competition between asperity flattening, which lowers the contact resistance and heating, which can affect the topography of the contact surface by the activation of thermal failure mechanisms. The stability of Au/Ru contact can then be helped by the lowering of material transfer because the contact materials are not softened. The low contact resistance of the Au/Ru contact could also be explain because this asymmetric contact includes a soft material and a harder one. The asperities of Au on the contact surface are more easily deformed due to the lower hardness compared to Ru. One assumption could be that the asperities of the softer material are much deformed by a hard material surface than a soft material one.

6. CONCLUSIONS

This new test facility enables new characterization tests of MEMS ohmic contacts under realistic conditions. The contact behaviour is typically multiphysic including mechanical, electrical and thermal interactions at the micro-contact interface. An emphasis was placed on the role of the low- to medium-power increase leading to contact heating. Various phenomena were observed as heating effects on contact resistance versus contact force dependence and the raw stabilization of the contact temperature from the softening. These mechanisms are commonly reported as failure vectors in the contact switch lifetime. Problems related to the softening of Au/Au and Ru/Ru electrodes are intimately related to the power handling capacity of the contact, which is limited by current density considerations. The main points revealed by these tests can be summarized as follow:

- The temperature rise induces contact softening. When the softening temperature is reached, the power dissipated in the contact contributes to anneal away the dislocations formed during plastic deformation.
- The softening of the contact surface is reached at ~ 3 mW for Au/Au contact and $\sim 4,25$ mW for Ru/Ru contact whereas the temperature of the Au/Ru contact is under the softening temperature at ~ 14 mW.
- The contact resistance becomes stable after reaching saturated regime with increasing force. This threshold is decreasing with increasing current level
- Au/Ru contact improved contact performance and enhanced power handling capability of the test structure thanks to electromechanical properties of the bimetallic contact configuration.

And finally, these tests bring to light the usability of this methodology to characterize the contact in term of reliability and performance under several test conditions. The knowledge gained is a better understanding of the contact physics in order to bring recommendations for further improvements of the contact reliability. The test vehicles used in this study could be also manufactured with various contact materials and several bump designs. The investigation of these two conception parameters is underway.

ACKNOWLEDGMENT

This work is supported by the ANR (Agence Nationale de la Recherche) in the frame of the FAME project.

REFERENCES

- [1] Solazzi, F. et al., "Contact Modelling of RF MEMS Switches Based On FEM Simulations", Proceedings of the 10th International Symposium on RF MEMS and RF Microsystems, pp 173-176, 2009
- [2] Fortini, A. and Mendelev, M.I. and Buldyrev, S. and Srolovitz, D., "Asperity contacts at the nanoscale : Comparison of Ru and Au", Journal of Applied Physics, vol. 104, no. 7, pp 074320.1-074320.8, 2008
- [3] Gilbert, K.W. and Mall, S. and Leedy, K.D. and Crawford, B., "A Nanoindenter Based Method for Studying MEMS Contact Switch Microcontacts", Proceedings of the 54th IEEE Holm Conference on Electrical Contacts, pp 137-144, 2008
- [4] Kwon, H. and Jang, S.S. and Park, Y.H. and Kim, T.S. and Kim, Y.D. and Nam, H.J. and Joo, Y.C., "Investigation of the electrical contact behaviours in Au-to-Au thin-film contacts for RF MEMS switches", Journal of Micromechanics and Microengineering no. 18, pp 1-9, 2008
- [5] Yang, Z. and Lichtenwalner, D. and Morris, A. and Menzel, S. and Nauenheim, C. and Gruverman, A. and Krim, J. and Kingon, A.I., "A new test facility for efficient evaluation of MEMS contact materials", Journal of Micromechanics and Microengineering no. 17, pp 1788-1795, 2007
- [6] Holm, R., "Electrical Contacts-Theory and Applications," 4th ed. Berlin Germany: Springer-Verlag, 1967.
- [7] Jensen, B.D. and Chow, LL and Huang, K. and Saitou, K. and Volakis, J.L. and Kurabayashi, K., "Effect of nanoscale heating on electrical transport in RF MEMS switch contacts," in Journal of Microelectromechanical Systems, vol. 14, no. 5, pp. 935-946, 2005.
- [8] Qing Ma, Quan Tran, Tsung-Kuan A. Chou, John Heck, Hanan Bar, Rishi Kant, and Valluri Rao, "Metal contact reliability of RF MEMS switches", Proc. SPIE, Vol. 6463, 2007.
- [9] Oliver, W.C., Pharr, G.M., "An Improved technique for determining hardness and elastic modulus using load and displacement sensing indentation experiments", J. Mater. Res., Vol. 7, No. 61992, 1992
- [10] Melle, S. and Dubuc, D.M.L. and Grenier, D. and Bary, K. and Plana, L. and Vendier, R. and Muraro, O. and Cazaux, J.L., "Modeling of the dielectric charging kinetic for capacitive RF-MEMS", IEEE MTT-S International Microwave Symposium digest, 2005
- [11] Segueineau, C., Desmarres, J-M., Dhennin, J., Lafontan, X., Ignat, M., "MEMS Reliability : Accurate Measurements of beam stiffness using nanoindentation techniques", Proceeding of CANEUS 2006, 27/09 – 1/10 06, 11057
- [12] Patton, ST and Zabinski, JS., "Fundamental studies of Au contacts in MEMS RF switches," in Tribology Letters, VOL. 18, pp 215-230, 2005.
- [13] Umemoto, T. and Takeuchi, T. and Tanaka, R., "The Behavior of Surface Oxide Film on Ruthenium and Rhodium Plated Contacts", IEEE Transactions on Components, Hybrids, and Manufactured Technology, vol. CHMT-1, no. 1, 1978
- [14] Feixiang Ke, Jianmin Miao and Oberhammer, J., "A ruthenium-based multi-metal contact RF MEMS switch with a corrugated diaphragm", IEEE/ASME Journal of Electromechanical Systems, vol. 17, no. 6, pp. 1447-1459, 2008.
- [15] Broue, A., Fourcade, T., Dhennin, J., Courtade, F., Dieppedale, C. , Pons, P., Lafontan, X, and Plana, R., "Validation of Bending Test by Nanoindentation for Micro-Contact Analysis of RF-MEMS Switches", 20th workshop on micromachining, micro mechanics and micro system, 2009